 DOI: 10.3217/978-3-99161-057-1-075

DFOS solutions covering full monitoring needs of an enlarged concrete deck viaduct

M. VILLAR[1], M. FERRARIO[2, 3], J. MOROSI[3]
[1] FEBUS Optics SAS, 2 Avenue du Président Pierre Angot 64000 Pau, France
[2] Politecnico di Milano, Department of Electronics, Information, and Bioengineering, Via Giuseppe Ponzio, 34, 20133 Milan, Italy
[3] Cohaerentia Srl, Via Pinturicchio 5, 20131 Milan, Italy.
Corresponding email: miguel.villar@febus-optics.com

ABSTRACT: 60s economic boom led to spread construction of large transport infrastructures. Many of these steel reinforced concrete structures attain their end of lifespans on this and next decade. With no major renewing plan, repairing and retrofitting are explored alternatives. A good example is Milano's ring-road viaduct; while already repaired and its concrete deck enlarged, SHM begins nowadays. **Monitoring of thermal and mechanical induced strain, static and dynamic, brings access to permanent strain, thermal expansion, eigenmodes of each single road span and better understanding of the whole structure dynamic behavior.** Three trucks moving at 30 km/h load dynamically the enlarged deck, while real traffic is used for modal analysis. Often, this kind of comprehensive monitoring requires combining various measurement technologies, making their installation time-consuming and expensive. Thus, the number of sensors may be undercut, and measurement campaigns duration reduced, which may result in poorer monitoring results and mismatching between experimental results and model's ones. FEBUS SHM solutions based on DAS (Distributed Acoustic Sensing), DSS (Distributed Strain Sensing) and DTS (Distributed Temperature Sensing) provide quick instrumentation and easy monitoring. With long-range devices to address tens of km of infrastructure instrumented in a row, up to 400 kHz continuous monitoring, state-of-the-art DAS repeatability threshold of only 2 picoStrain/SquareRoot(Freq), FEBUS DFOS (Distributed Fiber Optics Sensing) solutions brings values for every node of the structure, remote monitoring and mastered opex and capex.

KEY WORDS: SHM; DFOS; DAS; Bridge monitoring; Dynamic strain monitoring; Fiber Optics instrumentation.

1 INTRODUCTION

DFOS begins to play a major role in SHM due to its outstanding combination of huge number of sensing points, sensitivity, repeatability, and easiness of very large instrumentation. In the pastr, DAS (Distributed Acoustic Sensing based on Rayleigh Backscattering in fiber optics) has been used to assess the dynamic behavior of a structure, while DSS/DTS (Distributed Strain Sensing / Distributed Temperature Sensing both based on Brillouin backscattering in fiber optics) focused on quasi-static strain and temperature monitoring.
The collapses of widely used infrastructures like the Morandi Bridge in Genoa and the Florida International University Pedestrian Bridge have highlighted the need of implementing monitoring strategies to prevent such disasters. These failures are often attributed to design flaws, material deficiencies, overloading, or insufficient maintenance. Following the Morandi bridge collapse, a substantial number of infrastructures were flagged for close inspection. DFOS monitoring can play a major role in detecting anomalies and raising early alerts to infrastructure operators and owners before collapses occur. Indeed, traditional point sensors have limitations, especially in urban environments with complex needs, stacked infrastructures and embedded networks [1 - 7].
When addressing Operative Modal Analysis, we can benefit from high sensitivity of DAS, and different kind of active and passive sources can be used. Indeed, Ambient vibration recordings provide valuable dynamic information on structural behavior. These vibrations stem from various sources such as traffic on the deck and ambient anthropogenic noise, including external traffic, construction activities, and industrial operations, as well as natural elements like wind and earthquakes. They enable the estimation of dynamic parameters related to structural properties and serve as a valuable tool for monitoring structural condition [8 - 12].
This study shows how FEBUS Optics' DAS technology can be used for both dynamic (OMA) and quasi-static strain monitoring of an enlarged steel reinforced concrete bridge, which is a high-traffic viaduct.

Figure 1. Two in-parallel motorway steel reinforced concrete viaduct. Yellow lines show extended deck interface.

Indeed, the sensed structure is Milano's Ring-road, having a 12 km concrete viaduct with new bridge held by their own piles have been built parallel to each original viaduct and the road-

DOI: 10.3217/978-3-99161-057-1-075

slabs have been joined together through steel bars (Figure 1, Figure 2).

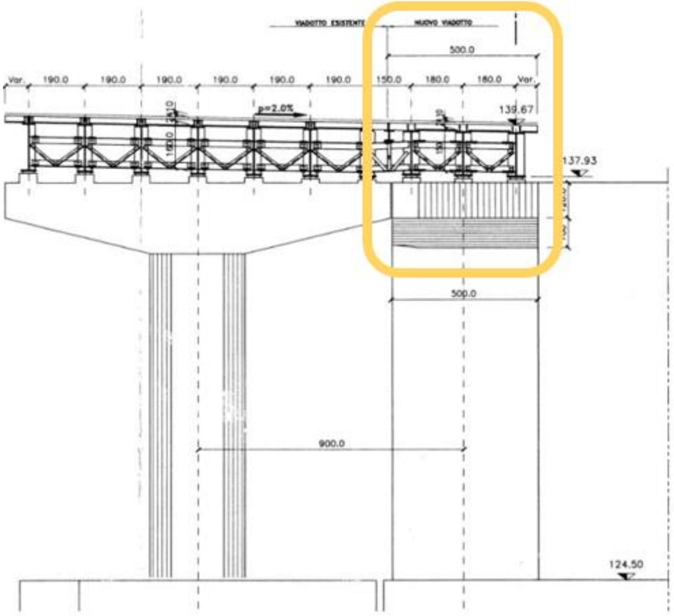

Figure 2. Transversal section. Extended deck in yellow frame

This viaduct is facing several issues and challenges. It is suffering from corrosion on its exposed rebars at several locations, not fully successful repair works, heavy traffic, and interferences with other infrastructures and buildings that complicate the attempts of structural retrofitting to improve safety and durability.

This study covers the first tests done with the initially instrumented parts of the viaduct and brought significant results to improve the understanding of the behavior of the structure, allowing to check the viability of the instrumentation for the entire viaduct, validating the numerical models, and highlighting the importance of monitoring and control of the structure to the asset operator (confidential).

2 METHODS

2.1 DAS. Distributed Acoustic Sensing

DFOS technologies rely on one of the three backscattering effects which are Rayleigh, Brillouin and Raman. The DAS (Distributed Acoustic Sensing based on Rayleigh backscattering technology) record high-frequency laser pulses sent into the fiber, analyzing backscattered light to detect heterogeneities along the cable.

Rayleigh backscattering, caused by defects in the fiber, is repetitive along its length and changes when the fiber is disturbed by external events. These changes grant access of physical parameters variations like vibrations coming from a leakage being energetic enough to propagate its related noise around. The optical phase shift between two positions along the fiber is related to the longitudinal strain using equation 1 below.

Key acquisition parameters include fiber length, pulse rate frequency, spatial and temporal sampling intervals, and gauge length (GL).

$$\varepsilon_{yy} = \frac{\lambda \cdot d\theta}{4\pi \cdot n \cdot GL \cdot \xi} \qquad (1)$$

Where ε_{yy} is the longitudinal strain, λ is the optical wavelength, dθ is the phase shift, n is the optical fiber index and ξ is a correction factor.

As briefly introduced above, the optical principle of operation is based on the Rayleigh backscattering of a light pulse propagating through the fiber. As it progresses, a tiny fraction of the laser pulse is continuously returned to the interrogator by random heterogeneities present in the fiber. An acoustic interaction at one point of the fiber will alter this process allowing its detection and location by time of flight of light (Figure 3).

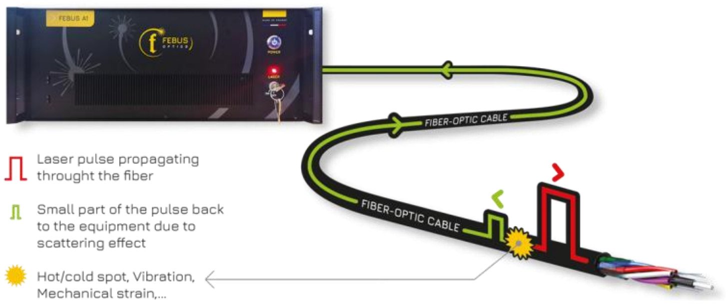

Figure 3. Principle of measurement via DFOS.

The information is contained in the optical phase of the received signal requiring interferometric detection. As the pulse propagates very quickly, the fiber can be repeatedly interrogated by sending a series of pulses, thus allowing to solve in frequency of acoustic vibrations (Figure 4) [13 – 17].

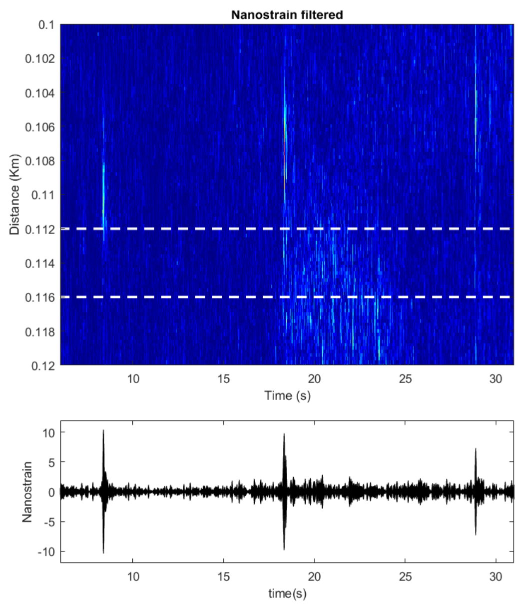

Figure 4. Distributed acoustic measurements. Filtered signal Bandpass @465Hz (Width 20Hz)

The achieved acoustic bandwidth can range from a few Hz to a few tens of kHz, the upper limit being a function of the length of the fiber used (the longer the fiber is, the longer the pulse will travel through the fiber and the lower the cut-off frequency is). This device performs highest state-of-the-art sensitivity,

DOI: 10.3217/978-3-99161-057-1-075

which is an advantage but can also be a disadvantage by being subject to noise acoustic environment. Real-time digital processing of the data is required to extract the signals of interest, as well as correctly applying the technology and instrumenting in the right manner the structure to be sensed. [18]

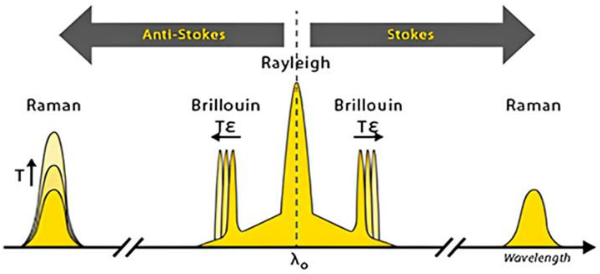

Figure 5. Fast Fourier Transform representation of Rayleigh, Brillouin and Raman backscattering [19]

2.2 *Experimental Setup. Dynamic loading of the viaduct*

Given the fact that the evolution of elastic modulus because of material ageing was not characterized and not having preliminary results from previous measurements at the beginning of this test campaign, one of the main challenges was to mobilize heavy enough loads to ensure the entire structure would strain as theoretically expected. To do so, up to three trucks were used to bend each span. The principle was very simple, each span was statically and dynamically strained by three trucks moving on single file at 30 km/h (Figure 6). Live tests were done overnight to be able to use these heavy trucks for loading.

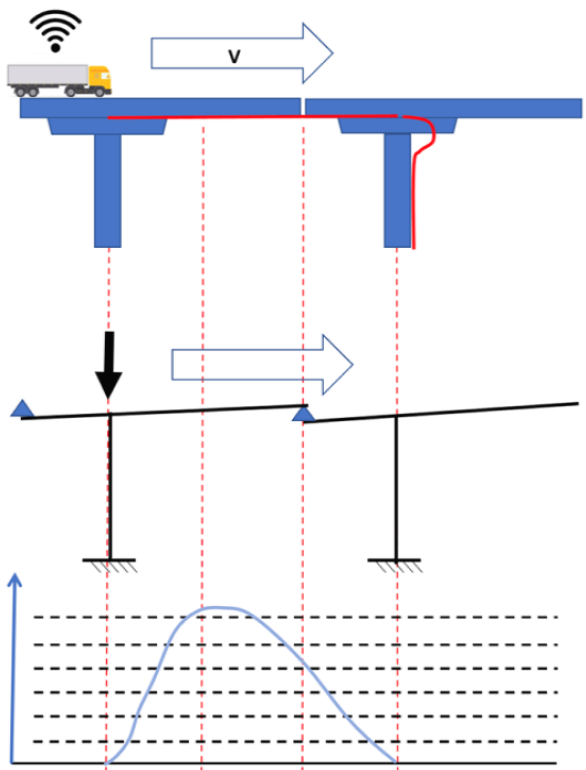

Figure 6. Principle of dynamic bending of viaduct's span.

Strain rate was measured by DAS. Both strain rate and dynamic strain were real-time plotted onsite. Indeed, time-integrated strain rate brings strain without need of classic DSS (Distributed Strain Sensing based on Brillouin). This use of Rayleigh backscattering technology (DAS) combines the best state-of-the-art repeatability of FEBUS A1 (DAS), the capability of measuring quasi-static strain and high frequency (up to 400 kHz) strain all along the sensing fiber optic cable which would be complex to match using Brillouin technology (DSS/DTS) going up to around 100Hz nowadays.

2.3 *Sensors. Fiber Optic sensing cables*

Three different fiber optic sensing cables were tested for this study.

- Strain sensing - Tight-buffered cable with steel reinforcement. Deemed the robust cable.
- Strain sensing - Tight-buffered cable without steel reinforcement. Lighter and less rigid providing more sensitivity but less protection.
- Temperature sensing - Loose tube cable. Essential to understand the thermal expansion of the viaduct. Not presented on this publication.

While choosing a robust (tensile, bending and torsion resistant) make sense for high demanding deployments, the downside is that cable reinforcements increase stiffness which tends to reduce sensitivity of the cable. That's why the second strain sensing tight-buffered cable without steel reinforcement is selected (Figure 7).
Additionally, temperature sensing loose tube cable is used for both assess the thermal behavior of the viaduct, typically sensing the temperature evolutions between day and night as well as seasons ones. This was used for a classic temperature compensation with other Brillouin interrogator used on the study but out of the scope of this paper.

2.4 *Instrumentation*

Different approaches were discussed during preparation phases. Indeed, one of the difficulties were to find a cost-effective method to instrument the entire viaduct in a durable and sensitive way. It is important to note that the instrumentation is done beneath the viaduct deck, under its bottom, so gravity is pulling down the whole cable/glue until fully cured. Prior the bonding, point-by-point attachments allow to place the cable at right position until the glue is spread and cured.
All the cables were bonded using three different glues:

- Fast crosslinking (*curing*) - Resin PPPO (2,5-diphenyl-p-phenylene oxide). Combining tenacity and vacuum effect to increase quick adherence (bonding strength).
- Strong – Thixotropic Polyurethane (undisclosed formulation). Extremely rigid after crosslinking. Specially designed for structural gluing.
- Medium Strong - Thixotropic Polyurethane (undisclosed formulation). Less rigid and quicker on crosslinking than the second one. Specially designed for structural gluing.

DOI: 10.3217/978-3-99161-057-1-075

Fast curing adhesive is used for the first part of the instrumentation. Despite the use of temporary tape, uncured state viscosity remains too low and not perfectly fully suited to bottom instrumentation. Main goal was to deem if coupling is severely impacted by the type of Strong and Medium Strong adhesives (Figure 7).

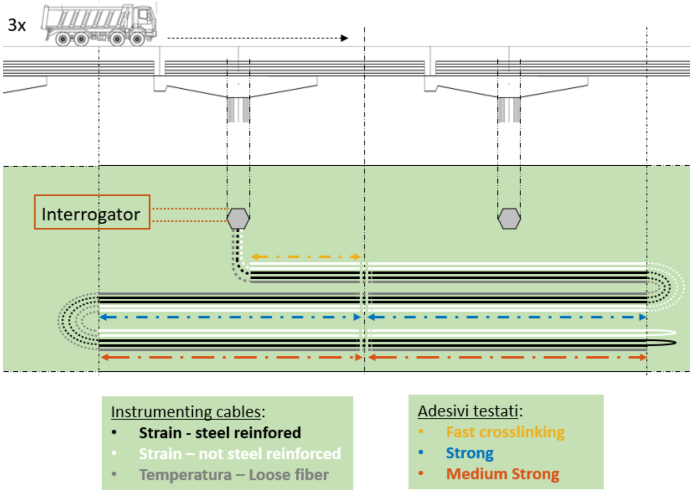

Figure 7. Sensors and Instrumentation.

Figure 7 shows the sensing fibers instrumentation in a single loop, so the full line is interrogated using only one channel. It is important to note during data interpretation that each cable passes three times through the same spatial point. This way, each truck will be seen three times.

3 RESULTS

3.1 Strain Rate monitoring

The results are presented on a 3-axis diagram typically called inverted waterfall. Time on vertical axis (sooner time close to zero), distance on horizontal axis and magnitude of strain Rate on colour scale on the right side (Figure 8).

The bending of the viaduct is properly captured. As expected, the tension relative strain (positive, red) appears first then replaced by compression (negative, blue) as truck goes away from each sensing point. This is coherent with a bended deck sensed on its bottom (Figure 6).

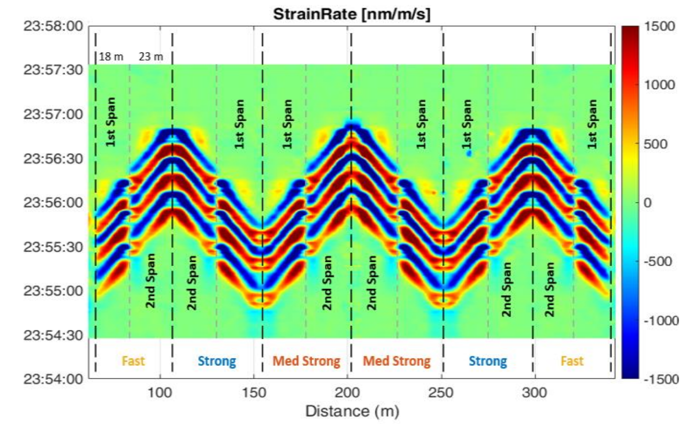

Figure 8. Longitudinal axis Strain Rate. Comparison of three different adhesives and two first instrumented spans.

It is noted the three trucks are equally captured. Indeed, three consecutive positive and negative loadings (related to (tensile and compression respectively) are plotted. Furthermore, the amount of strain is the same, meaning the three trucks weigh the same. Since the loads are moving at constant speed, both tension and compression strain rate follow constat slope. Trucks are moving in the same direction and sense; the wavy shape is due to the sensing fiber loop instrumentation (Figure 7). Both spans respond qualitatively and quantitatively in the same way. The same slope and same amount of strain rate around +/ 1500 nm/m/s. It is important to highlight the units (nanometers/meter/second) to understand the slight straining of the viaduct deck.

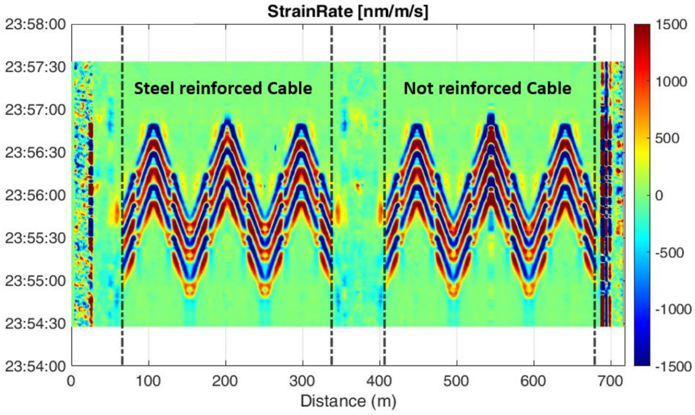

Figure 9. Longitudinal axis Strain Rate. Comparison of Steel reinforced and not reinforced cable.

Then, the adhesive and bonding are assessed. It is shown that all three adhesives show the same response. Indeed, there are no significant differences on the intensity of the strain rate which points to a similar coupling structure-sensors, leading *in fine* to a similar sensitivity. The same conclusion for the comparison between steel reinforced cable and not reinforced one, having similar sensitivity (Figure 9).

3.2 Strain monitoring

From previous results, strain rate expressed in nm/m/s - typical dimension and units of vibration on DAS measurements - many useful information can be inferred.

Dynamic strain rate can be time integrated to obtain strain, expressed on µm/m. In this case, typical integration time is 1ms but can be adjusted thanks to the capabilities of FEBUS A1 (DAS) to modify all its measurement parameters like pulse rate frequency (number of laser pulses emitted per time) and time resolution.

DOI: 10.3217/978-3-99161-057-1-075

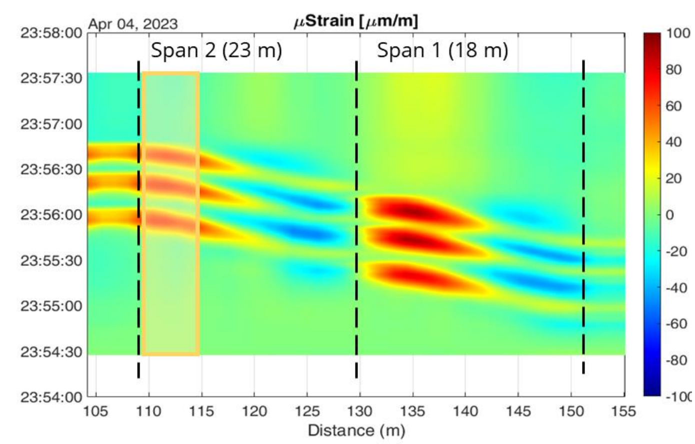

Figure 10. Longitudinal axis strain from time integrated strain rate

In the graph above (Figure 10), the strain is plotted in function of time (left axis) and distance (bottom axis), while intensity of the strain is represented by the color scale on the right. To enhance the result, only two first spans with strong glue are plotted. From 105 m to 155 m.

It is important to note the trucks are travelling from far distance to closer one, more precisely started on 155 m and go to 105 m, while the time is increasing on the left axis, so the trucks' movements is seen as diagonal from bottom right corner of the graph to the upper left corner.

It is observed in the figure above (Figure 10) the same patterns of positive and negative strain for each truck pass, as seen with strain rate. In contrast of strain rate results exploitation, we can note that the first span is reaching up to 100 µm/m on tensile and -60 µm/m on compression, while the second span is less strained on tensile, going up to 80 only µm/m, and the same compression strain of -60 µm/m.

To go further in the quantification, we can see the pass of the trucks two and three on second span seemed to load 20 µm/m more than the pass of the first truck.

3.3 Displacement monitoring

It is important to note that one the main aim of this study was to quantify the positive longitudinal displacement of the span because of the bending. To do so, a space integration was done at a particular point, where the strain was related to tensile, so positive. The region of this point is represented by the orange rectangle between 110 m and 115 m (Figure 10).

Longitudinal axis displacement

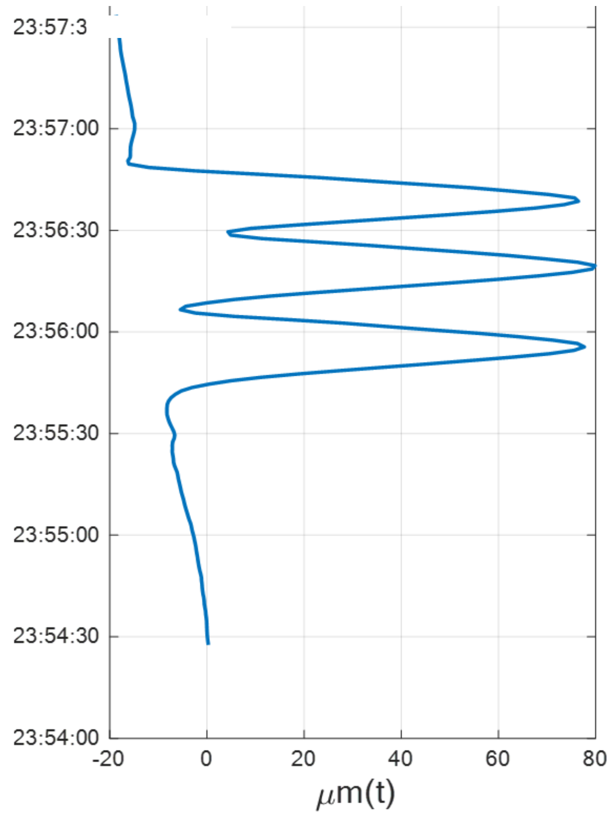

Figure 11. Longitudinal axis displacement from space integrated strain

In the graph above (Figure 11), we can see the result of the space integration of the strain rate, which is the longitudinal axis displacement created by the bending of the span. The length of integration was 1m, which can be tuned as wished with FEBUS A1. Thus, it is observed the amount of displacement is 80 µm/m on first span. This matches the expectations from numerical modelling as confirmed by the technical direction of CaeMATE Srl, the entity tasked of the mechanical modelling of the bridge for this study.

3.4 Modal analysis with DAS

FEBUS A1 DAS was applied for monitoring of strain rate, strain and displacement but also for its more common use, modal analysis. The same cable and interrogator were suited for this kind of acquisition, and the real traffic at a high load time of the day (rush hour) was used. This is widely used and bring plenty of acoustic signals. Since the sensitivity of DAS is very high, it is preferable to plot results at one single point but other FFT-based 3D representations allow to get info from the entire line at once. In this case, the choice is to represent time on left axis while the frequency is on the bottom axis, while color represents the signal energy, thus amplitude of the vibration (Figure 12).

DOI: 10.3217/978-3-99161-057-1-075

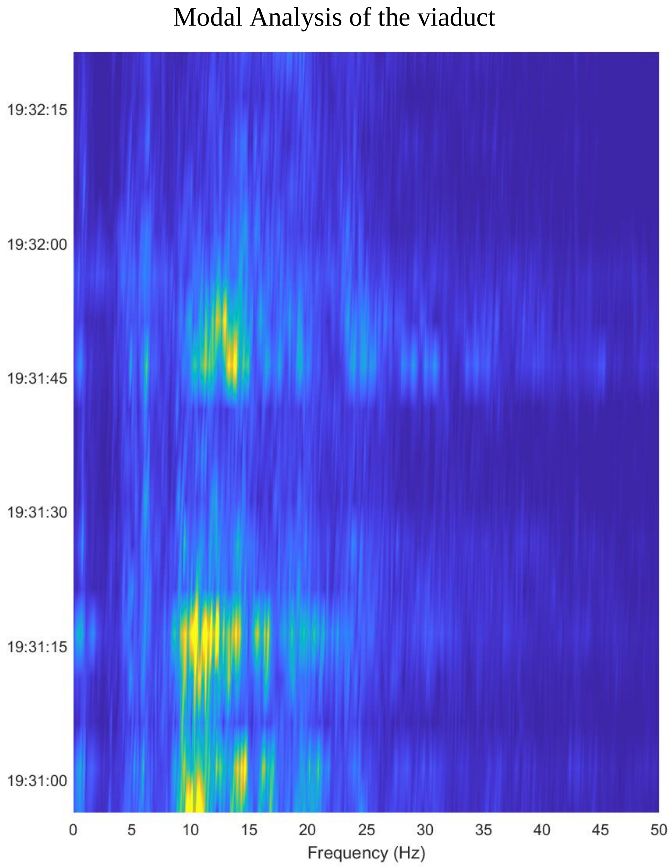

Figure 12. Vibrations from real traffic, frequency in function of time for a particular point

From previous information, the frequencies can be represented for a particular point and time, thus the amplitude of the vibration in function of the frequency, as shown on the figure below (Figure 13). In the aim of comparison of different states, two instants are plotted, on red the steady state to see the ambient noise when no vehicle on the instrumented spans, and blue for high intensity signals from traffic on the instrumented spans.

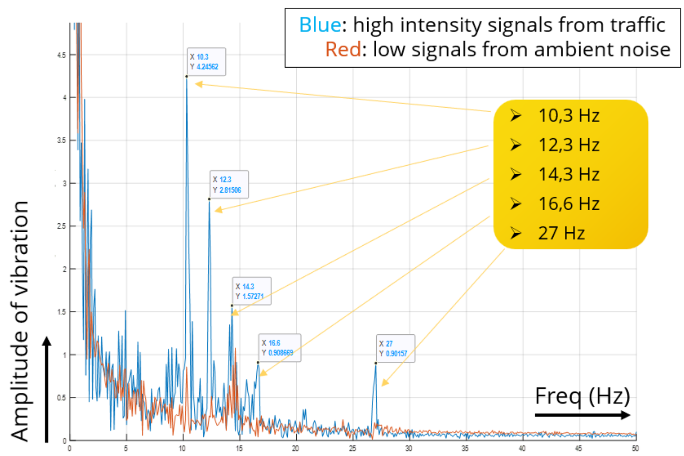

Figure 13. Modal frequencies of the viaduct

Up to five modal frequencies are detected clearly, between 10,3 Hz and 27 Hz.

It is important to note that this is plotted for one single point, thus one node identified previously on FFT over distance, but it is possible to do the same analysis for all the nodes of the structure, that are sensed simultaneously thanks to the properties of Distributed Acoustic Sensing, and its long range and fine resolution measuring capabilities.

4 DISCUSSION

It has been shown that DAS technology can be applied to both dynamic and quasi-static acquisitions addressing OMA and strain measurements with the same sensor (Fiber Optics) and DAS interrogator (FEBUS A1). Live data production - time and space integration - allowed to go from strain rate to strain and displacement during the acquisitions and check the quality of results and the coherence with the numerical models.

While this is mathematically well known, the application of this methodology to DAS acquisitions is a novelty that unlocks new applications of DAS in the context of SHM and Civil Engineering as well as other potential uses on sectors like Oil & Gas and Geophysics, for static and dynamic assessment of pipelines and ground movement for instance. Indeed, thanks to the capabilities of FEBUS A1, all measurement parameters can be easily modified to suit to the infrastructure length and acquisition demands.

Besides, one of the main advantages of Modal analysis of DAS monitoring is the possibility to combine high sensitivity and decide the position of nodes after instrumentation, allowing to overcome the difficulties of predicting the nodes of the vibration modes, and deciding the right positions to locate traditional point sensors without knowing how the structure behaves dynamically. For the selected position, 5 modal frequencies were located spectrally and quantified in terms of amplitude of vibration.

The measurements were achieved with all the combinations of cable and adhesive in the scope, two different cables, steel reinforced and not reinforced, and three different glues. Indeed, all cables and glues tested shown good properties in terms of coupling and sensitivity for the intended goal of longitudinal axis displacement and Modal Analysis.

ACKNOWLEDGMENTS

Prof. Mario Martinelli, Maddalena Ferrario, Jacopo Morosi and their team for the work on preparation, instrumentation and sharing data.

University Politecnico di Milano and its Department of Electronics, Information, and Bioengineering, as well as Cohaerentia Srl for the logistics and support during the preparation and first data analysis.

CaeMATE Srl for assisting the overnight tests and giving feedback from their theoretical models.

The operator of the infrastructure (undisclosed name - confidential) for granting access to their viaduct and allowing the overnight measurements with heavy trucks.

REFERENCES

[1] Calvi, G. M., Moratti, M., O'Reilly, G. J., Scattarreggia, N., Monteiro, R., Malomo, D., ... & Pinho, R. (2019). Once upon a time in Italy: The tale of the Morandi Bridge. Structural Engineering International, 29(2), 198-

DOI: 10.3217/978-3-99161-057-1-075

217.

[2] Cao, R., El-Tawil, S., & Agrawal, A. K. (2020). Miami pedestrian bridge collapse: Computational forensic analysis. Journal of Bridge Engineering, 25(1), 04019134.

[3] Figueiredo, E., & Brownjohn, J. (2022). Three decades of statistical pattern recognition paradigm for SHM of bridges. Structural Health Monitoring, 21(6), 3018-3054.

[4] Maurey, H., Chaize, P., & Dagbert, M. (2019). Sécurité des ponts : Éviter un drame.

[5] Anastasopoulos, D., De Roeck, G., & Reynders, E. P. (2021). One-year operational modal analysis of a steel bridge from high-resolution macrostrain monitoring: Influence of temperature vs. retrofitting. Mechanical Systems and Signal Processing, 161, 107951.

[6] Khoo, L. M., Mantena, P. R., & Jadhav, P. (2004). Structural damage assessment using vibration modalanalysis. Structural Health Monitoring, 3(2), 177-194.

[7] Snover, D., Johnson, C. W., Bianco, M. J., & Gerstoft, P. (2021). Deep clustering to identify sources of urban seismic noise in Long Beach, California. Seismological Society of America, 92(2A), 1011-1022.

[8] Peeters, B., & De Roeck, G. (2001). One-year monitoring of the Z24-Bridge: environmental effects versus damage events. Earthquake engineering & structural dynamics, 30(2), 149-171.

[9] Magalhães, F., Cunha, Á., & Caetano, E. (2008). Dynamic monitoring of a long span arch bridge. Engineering Structures, 30(11), 3034-3044.

[10] Farrar, C. R., Doebling, S. W., & Nix, D. A. (2001). Vibration–based structural damage identification. Philosophical Transactions of the Royal Society of London. Series A: Mathematical, Physical and Engineering Sciences, 359(1778), 131-149.

[11] Magalhães, F., Cunha, Á., & Caetano, E. (2012). Vibration based structural health monitoring of an arch bridge: From automated OMA to damage detection. Mechanical Systems and signal processing, 28, 212-228.

[12] Rodet J., Tauzin B., Amin Panah M., Gueguen P., Nziengui BA D., Coutan O., Brule S. (2024). Urban dark fiber Distributed Acoustic Sensing for bridge monitoring. E-Journal of Nondestructive Testing - July 2024. ISSN 1425-4934.

[13] Hartog, A. H. (2018) An Introduction to Distributed Optical Fibre Sensors. CRC Press 2018-06-28.

[14] Tanimola, F., & Hill, D. (2009). Distributed fibre optic sensors for pipeline protection. Journal of Natural Gas Science and Engineering, 1(4-5), 134-143.

[15] Fichtner, A., Bogris, A., Nikas, T., Bowden, D., Lentas, K., Melis, N. S., ... & Smolinski, K. (2022). Theory of phase transmission fibre-optic deformation sensing. Geophysical Journal International, 231(2), 1031-1039.

[16] Froggatt, M., Soller, B., Gifford, D., & Wolfe, M. (2004, February). Correlation and keying of Rayleigh scatter for loss and temperature sensing in parallel optical networks. In Optical fiber communication conference (p. PD17). Optica Publishing Group.

[17] Gifford, D. K., Kreger, S. T., Sang, A. K., Froggatt, M. E., Duncan, R. G., Wolfe, M. S., & Soller, B. J. (2007, October). Swept-wavelength interferometric interrogation of fiber Rayleigh scatter for distributed sensing applications. In Fiber Optic Sensors and Applications V (Vol. 6770, pp. 106-114). SPIE

[18] Huynh C. Real-Time Classification of Anthropogenic Seismic Sources from Distributed Acoustic Sensing Data: Application for Pipeline Monitoring

[19] https://www.febus-optics.com/fr/page/technology.